FEM ANALYSIS OF A BELT CONVEYOR DRIVING DRUM

[1]A. Mihailidis, [1]E. Bouras*, [1]E. Athanasopoulos
[1] Aristotle University of Thessaloniki, Greece

KEYWORDS –BELT CONVEYOR, THIN WALLED STRUCTURE, FE MODEL

ABSTRACT –
Large scale belt conveyor systems have a lot of unique characteristics, such as long conveying distance, large capacity and high efficiency, continuous transportation of bulk materials as well as central control and management. The motion of the belt conveyor system is controlled by a driving station, which consists mainly of two driving pulleys and one pre-tensioning pulley. The pulley drums are thin walled structures produced by rolling a thick steel sheet and welding it with two end plates. Decreased service life has been observe in the open mine of Amyntaion Greece, resulting in frequent break downs. Drum replacement in the harsh muddy conditions stalls the operation of the belt systems up to two days. In addition to the cost of the drum, it results in a dangerous and financially cumbersome repair. The drums are subjected to variable loads depending on weather, pretension and mined material. Therefore a methodology for modelling, which would take all these into consideration was necessary. In the current study, the aim is to test various load scenarios on a reinforced drum model and compare the results against the two types currently in service. Modelling the complete pulley assembly is the currently accepted method for drum analysis, since the stiffness is influenced by the shaft due to the locking connecting components used. The force application utilizes a user selectable distribution function along the axis of the drum and the Euler's belt formula along the circumference. The models were built in ANSA, and optimized in terms of mesh density around the high load areas, while built-in pressure distribution tools and python scripting were utilized to apply the load case.

Nomenclature:

D : Drum outside diameter [m]
F_S : Bearing force acting of the pulley shaft [N]
F_1 : Force of the tight span [N]
F_2 : Force of the slack span [N]
T_{tot} : Total torque applied to the pulley shaft [Nm]
α : Contact angle measured from the belt entry point [deg]
α_G : Sliding angle [deg]
μ : Friction coefficient of the belt on the drum surface
μ_{min} : Minimum friction coefficient required to avoid sliding of the belt on the drum surface
φ : Angle measured from the belt entry point [deg]
r : Radius of the drum shell [m]
L : Width of the drum [m]
z : Position along the axis, measured from the drum mid-plane
P(α,z) : Element pressure as a function of circumferential and axial position
A,B : Factors used in load distribution

1. INTRODUCTION

Open mines are a vital part in the production chain of electricity used in Greece operated by the Public Power Corporation S.A. (P.P.C). Greece ranks 4th in coal production in E.U [1] according to EURACOAL and 5th in the world. The surface strip mines in the Lignite Centre of Western Macedonia are the biggest in the Balkans, with the Amyntaion mine being the 3rd out of the 5 in this area having a yearly production of 8-9 10^6 t of coal while excavating over 50 10^6 t of earth. All mined materials are transported towards either the deposition area or the power plant via large-scale belt conveyor systems. They offer high efficiency along with central control and continuous operation. The Amyntaion mine shown in Figure 1, has an

installed belt system measuring 22 km, consisting of 50 independent belt drives. Their supply rate reaches over 19,000 t/h. The mine is over 220 m deep, constantly expanding, which results in inclination reaching over 12.2% for the belt conveyor systems. Each individual conveyor system consists of the driving head station, the belt and a tail station. The driving head is depicted in Figure 2 and consists of two driving pulleys and a pre-tensioning one. Each driving pulley is powered by two synchronous motors (one at each side) rated at 1250 kW at 988 rpm each. Each motor transmits its power through a two stage gear reducer with a total transmission ratio *i*=14.78 resulting in a linear belt velocity of 5.25 m/s. The bearing forces are captured and recorded by two load cells on the basis of the rear driving pulley.

Figure 1 **–** Overview of the Amynteon strip mine. The largest continuous conveyor is distinguishable in the middle having a length of over 2km.

Tension pulley

Rear driving pulley

Figure 2 – A head driving station, driving and tensioning drums

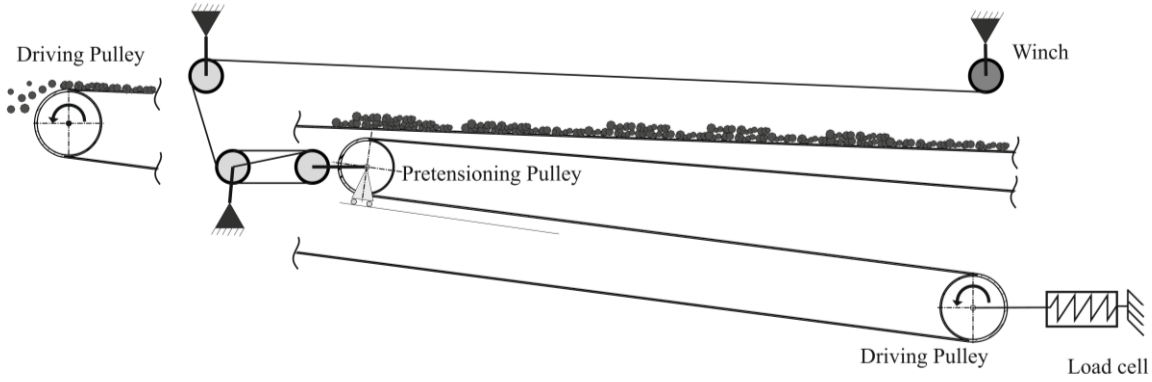

Figure 3 – An overview of the path and components inside a driving head station

Due to the widespread usage of belt conveyor systems worldwide, their design has been the topic of extensive research. Analytical methods were originally developed due to their fast and cost-effective application. FE method was deemed more appropriate since the

integration of all the components has a significant influence in the service life. Due to the high cost of the FE method, it was not favoured by the pulley manufactures that are commonly tasked also with the design. Since the rapid decrease of processing power cost and associated speed increase, FE is nowadays commonly employed.
Already from 1963 in the work of Lange [2] a significant number of drum variants were in operation. Despite that, even today the subject remains open. Lange aimed to create an analytical method to calculate the stresses on the shell of the drum. The triaxial stress state on the shell and end discs were represented as Fourier series. In an effort to improve end plate stress, drum reinforcement with a mid-plane diaphragm was studied by Kalikhman and Umanskii [3, 4]. Using analytical methods in the reinforced drum, they showed that the mid-plane diaphragm reduces the occurring stress. They additionally measured in a test rig the stress at several spots. Good agreement at high loads was shown but due to limitations of the test method, results showed discrepancies at low loads. Schmoltzi [5] in 1974 calculated the stress field in the pulley taking into account the effect of the keyless locking assemblies that replaced the previously welded hubs. He tested five different types of drums over different loads in a test rig and measured the developed stress at several points, while comparing the results with the analytical solutions.
In 1985, one of the first FE method application on drums was done by King [6]. He validated the results against the analytically obtained and a measurable difference was found. Based on the results he proposed the “L” bottom versus the “T” bottom endplates in order to minimize the machining cost while lowering the stresses on the welds. A decade later Sethi and Nordell [7] evaluated a great variety of pulley designs using the FE method. In addition to this, Qiu and Sethi [8] presented a pulley stress analysis method based on reformatted transfer matrix, in order to validate the accuracy of the FE method. Ravikumar and Chattopadhyay [9] in 1999 developed a semi-analytic finite element software utilizing a 3-noded thick conical shell and a triangular ring element. They studied the pulley as an integral structure and managed to show the mutual interdependence of the pulley components.
The advent of advanced modelling tools has allowed researchers to model in greater detail not only 2D axisymmetric slices but complete 3D assemblies of thousands of elements. Welds began to be incorporated in the FE models. Affolter *et al*. [10] studied the failure of a drum weld, and remarked on the necessity of reinforced connection between the end plates and the shell. They calculated the stress field using a FE model according to the FKM [11] guidelines while utilizing symmetry to reduce the size. They concluded that start-up loads can be decisive for dimensioning and manufacturing tolerances should be considered. Lill [12] in 2007 supported the use of FE method for calculation since rule of thumb failed to correctly calculate the loads. Furthermore, limits provided in BS 7608 [13] regarding welds must be adhered during design. The initial assumptions of the belt load, that the load is uniformly applied is challenged and more accurate modelling was tested. Wang *et al*. [14] in 2011, incorporated in their analysis the belt-pulley contact model by simulating the belt as a steel structure with the equivalent thickness. Styger and Laubscher [15] 2011 analysed a quarter model of a pulley, applying the necessary boundary conditions and using 3D linear hexahedral elements. Using a semi-analytic method they calculated the axisymmetric quarter model and validated the accuracy of the FE results. Additionally, they took into account the residual stresses due to the welding process, which they measured with the hole drill method. Yong-cun *et al*. [16] in 2012 created a parametric tool for designing drums and meshing them in a wizard like automated form. Wu and Guan [17] also created a parametric tool for designing drums ready to be used in a FEM analysis with post-processing. The load distribution on the model was done by curve fitting a second order polynomial in the radial direction. Yuan *et al* [18] 2014 presented an objective function comprised of main design parameters of a drum in order to optimize the design of drums. Using FEM software and mathematical packages they optimized in a driven drum, the bearing position.

2. MODEL DESCRIPTION

Pulley design

The drum is made of 32 mm thick plain steel sheet and is welded to the plate ends. The shaft is connected by keyless locking assemblies. The outside diameter of the drum is 1500 mm and the width 2600 mm. The reinforcing is a 30 mm thick mid-plane diaphragm as shown in Figure 4.

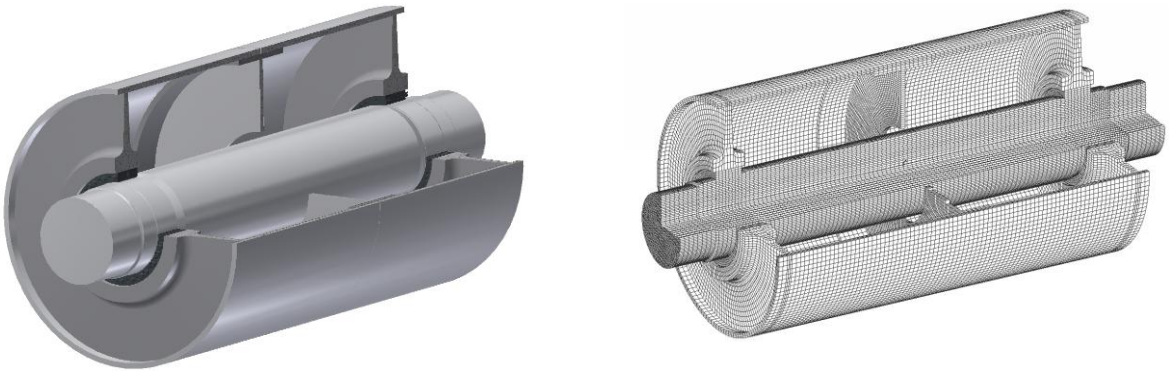

Figure 4 – The CAD model (left) of the drum. The FEM mesh as created by HEXABLOCK in ANSA.

Finite element modelling

The model as shown in Figure 4 includes the major components of the assembly while simplifying some connections. The FE model includes the drum, both endplates and mid-plane diaphragm, the shaft and the locking assemblies. The connection between the shaft and the locking assemblies was modelled as tied nodes, while the welds were modelled as unified components. The shaft was supported by MPCs at the bearings seats. At one side, the centre node of the MPCs was able to rotate and slide, while on the opposite it was fixed and allowed only to rotate. The preparation of the finite element models was done using the ANSA [19] pre-processor, while the post-processing and evaluation of the results were performed in μETA [20].

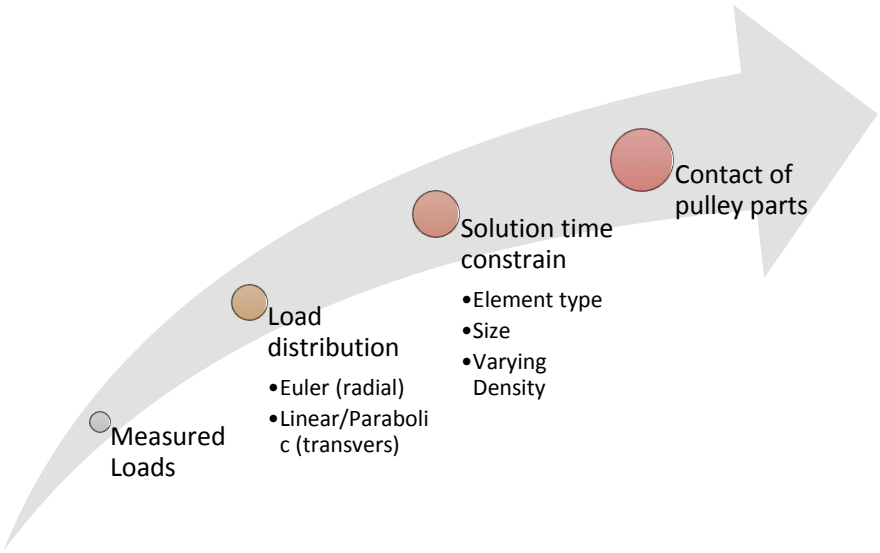

Figure 5 – Evolution of the modelling process

The main disadvantage of such methods is the increased execution time. A goal of the present study was to counter this by placing constrains regarding the preparation and solution time within a feasible timeframe for the industry. The aim, as shown in Figure 5, is to evolve a process that can provide quick and reliable results. Initially a 2D shell element model was setup, using mid-surface extraction from within ANSA. The number of elements and the resulting solution time was compared to the equivalent model using 3D elements. The use of the 3D elements had a marginal impact on solution time but significantly increased the accuracy. The 2D mesh was abandoned and all models afterwards were done with 3D solid elements.
For getting better results on the areas of importance, the drum and the diaphragm were meshed using the MAP function. The end plates, due to complex geometries, were meshed using the HEXABLOCK tools of ANSA. The keyless locking assemblies used to connect the shaft and the end plates were modelled as solid blocks. The shaft was the only component of the model that contained PENTA elements, as the part of the minor importance. Nevertheless, modelling the elastic behaviour of the shaft had large impact on the accuracy of the analysis. The initial 3D model of the reinforced drum had 287,296 HEXA elements, 15,372 PENTA elements and a total of 326,436 nodes. The model had an overall element length of 30 mm. The convergence validation of the calculated stress field was necessary and therefore three alternative element lengths were used. The increasing number of elements results in disproportionate time increase. Two strategies were used to control the increase. A variable density along the drum and a switch from HEXAS that require prolonged preparation time to TETRAS. The loss of result accuracy is known, but the solution aims at producing a fast solution to assist in design while having adequate resolution near the high stress points.
A similar drum model with smaller dimensions was build and solved in order to estimate the solution convergence. The FE models are shown in Figure 5. Scaling the magnitude of the elements appropriately the larger and complete model was then solved. In the same model the introduction of contact between the end-plates and the drum was examined. Due to manufacturing errors, small gaps can be present between the bodies.

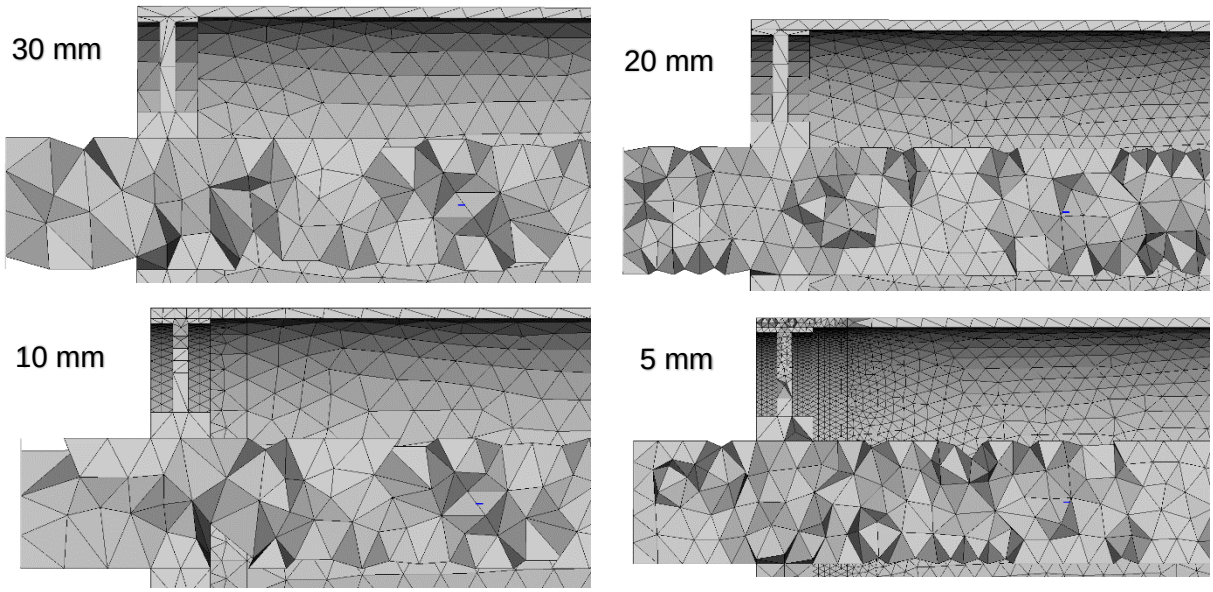

Figure 5 – Four different mesh densities and locally variable density.

The models were solved utilizing the implicit ABAQUS solver and the resulting stress fields were visualized using the META software developed by BETA CAE.

Load distribution of a drum

In steady state operation, a number of loads are acting upon the drum;

a) the normal (i.e. radial) and friction (i.e. tangential) force applied by the belt,

b) the torque and bearing forces applied on the shaft from the synchronous motors and the rolling element bearings.

Two models are commonly used regarding the interaction between belt and drum. The first, called the creep model, was developed by Euler, assumes that the existence of friction depends entirely on the relative motion (creep) of the belt on the drum surface. It is widely adopted in industrial applications. The second model, called the shear model, uses a more realistic representation of the belt. The belt is assumed to be of pliable elastomer with embedded high strength cords. Therefore, it adheres on the surface as long as the shear is less than the maximum friction force. Comparisons between the two models [21] showed that the distribution of the belt tension and friction over the belt-drum contact arc are markedly different. Although the shear model seems closer to modern drives, the adoption of the creep model for the current case is justified since it allows a safer estimation.
The belt forces on the two branches of the belt wrapped around the pulley are calculated from the total input torque and the bearing forces. These parameters were measured on-site over a period of time using the ampere-meter readouts and two load cells shown in Figure 3. The radial distribution of the resulting normal and friction forces depends on the friction coefficient of the belt on the drum surface, which is unknown and difficult to estimate because it depends on many parameters, such as humidity, temperature and surface condition. A rather typical value of friction coefficient is μ = 0.75. In this case, the sliding angle α_G is given also by the Euler formula:

$$F_1 = \frac{F_s}{2} + \frac{T_{tot}}{D} \tag{1}$$

$$F_2 = \frac{F_s}{2} - \frac{T_{tot}}{D} \tag{2}$$

$$e^{\mu \cdot \frac{a_G \cdot \pi}{180}} = \frac{F_1}{F_2} \Rightarrow e^{\frac{0.75 a_G \cdot \pi}{180}} = \frac{F_1}{F_2} \tag{3}$$

The distribution of the load in the axial direction of the drum is not unanimously agreed upon the researchers, with a number of different models. The classical and simpler to model is the uniform distribution of the forces along the belt. Alternative models have been used such as sinusoidal of various degrees, second order polynomial as well as edge loaded linear. Assuming a cylindrical coordinate system in ANSA with centre, the centre of the pulley, the nodes can be defined by the pair (α,z). The sum of all loads acting on the surface must be equal to all acting forces on the cylinder. Using the equation in Table 1 the pressure as a function of the angle a and the width z can be calculated for all nodes. The function parameters have to be evaluated by solving the integral (eq. 4) on the area and equating that to the total forces applied.

$$\int_{z=-\frac{L}{2}}^{z=\frac{L}{2}} P_{linear}(a,z)\, dz = \int_{z=-\frac{L}{2}}^{z=\frac{L}{2}} P_{parab}(a,z)\, dz = Po(a) * L \tag{4}$$

The complete equation is then used with the DLOAD functionality available in ANSA and applied on a node set that contains 180 degrees of the outer surface of the drum. The a and z variables in ANSA can be inserted as “yelc(@EID@,1)” and “zelc(@EID@,1)” respectively, where 1 is the specific cylindrical coordinate system.

P(a,z)	Stick	Slip
Uniform	$\frac{F_1}{L \cdot r}$	$F_2 \frac{e^{\mu \cdot (180-\alpha) \cdot \frac{\pi}{180}}}{L \cdot r}$
Linear	$\frac{F_1}{L \cdot r}$	$A \cdot z + F_2 \frac{e^{\mu \cdot (180-\alpha) \cdot \frac{\pi}{180}}}{L \cdot r}$

Parabolic	$(A \cdot z^2 + B)\frac{F_1}{L \cdot r}$	$(A \cdot z^2 + B)F_2\frac{e^{\mu \cdot (180-\alpha)\cdot \frac{\pi}{180}}}{L \cdot r}$

Table 1 – Force distribution equations.

The resulting force diagrams are shown in Figure 6 in a cross-section of the drum, and in Figure 7 over the applicable area.

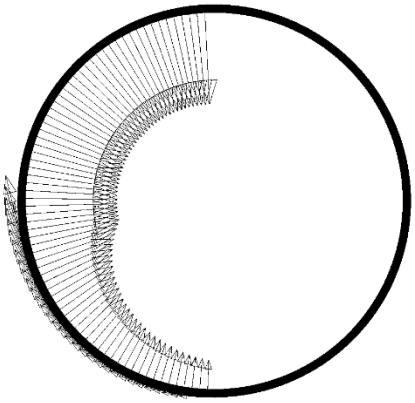

Figure 6 - Euler distribution

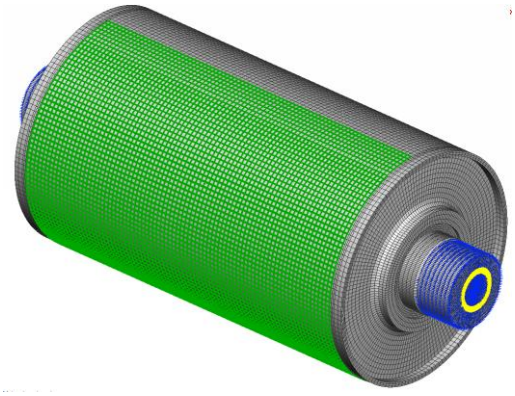

Figure 7 - Node set of drum

3. RESULTS

Influence of mesh density

Using the smaller model, the dependence of the stress field to the mesh density is observed. In Figures 8, 9, the end-plates of the smaller test model were meshed with three different densities and subjected to the same loading conditions. The maximum stress converges from the 10 mm element and lower, while using 5 mm results in some benefits regarding the contact. Using the information gained, the right column of tests was performed to evaluate the influence of a large element length on the symmetrical portion of the drum. Using the 10 mm along with a very rough mesh on the symmetrical part influenced the results, while a ratio of 5 to 20 mm had negligible effect on the stress field.

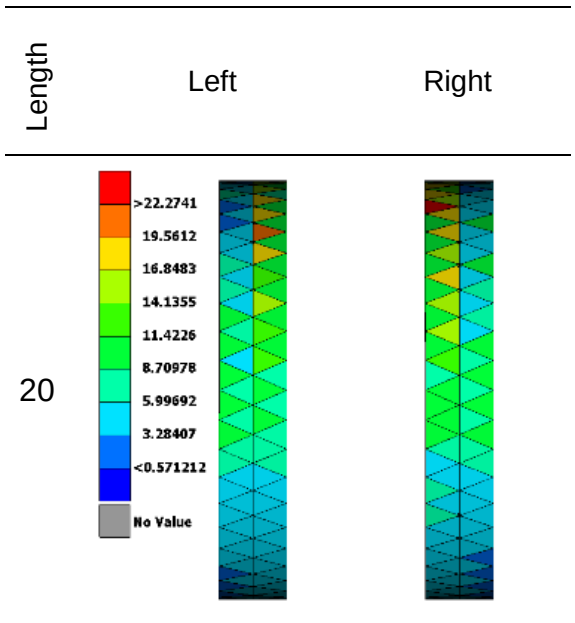

Figure 8 – Uniform mesh density of both ends of the drum.

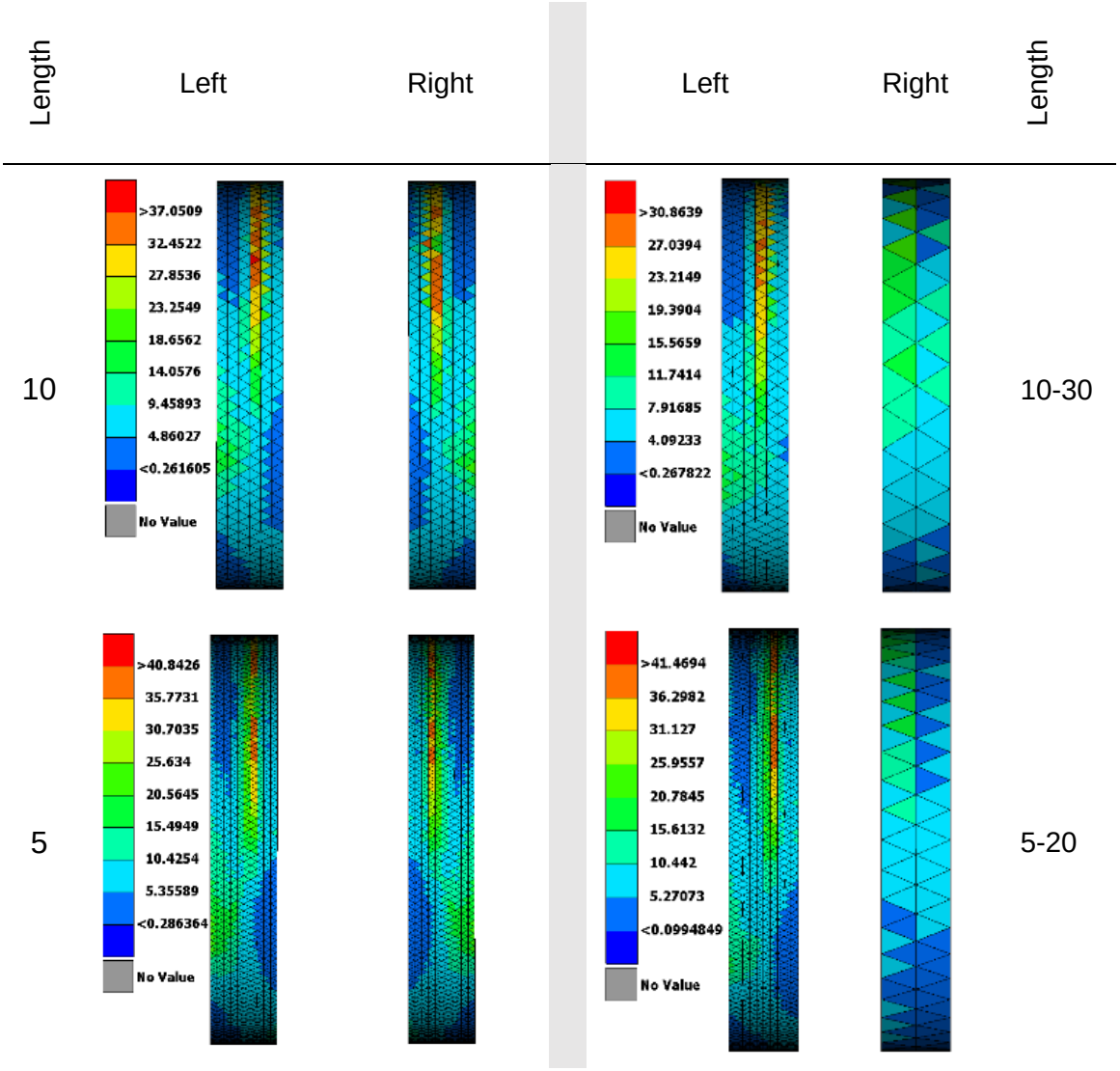

Figure 9 – Variable mesh density (left) and differentiation of the symmetrical mesh (right) on the right side of the drum

Influence of force distribution

The force distribution is shown in Figure 10 overlaid (in white) on the resulting stress of the shell. The linear force distribution used is a result of the maximum difference measured between the load cells. The values for the bearing force had a difference of 40 tons. The parabolic is closer to the sinusoidal distribution presented in the literature. It results in more favourable stress field since the reinforcement diaphragm is loaded significantly while the positions of maximum stress moves towards the inside. The three distributions are compared in Figure 11 over the same row of elements.

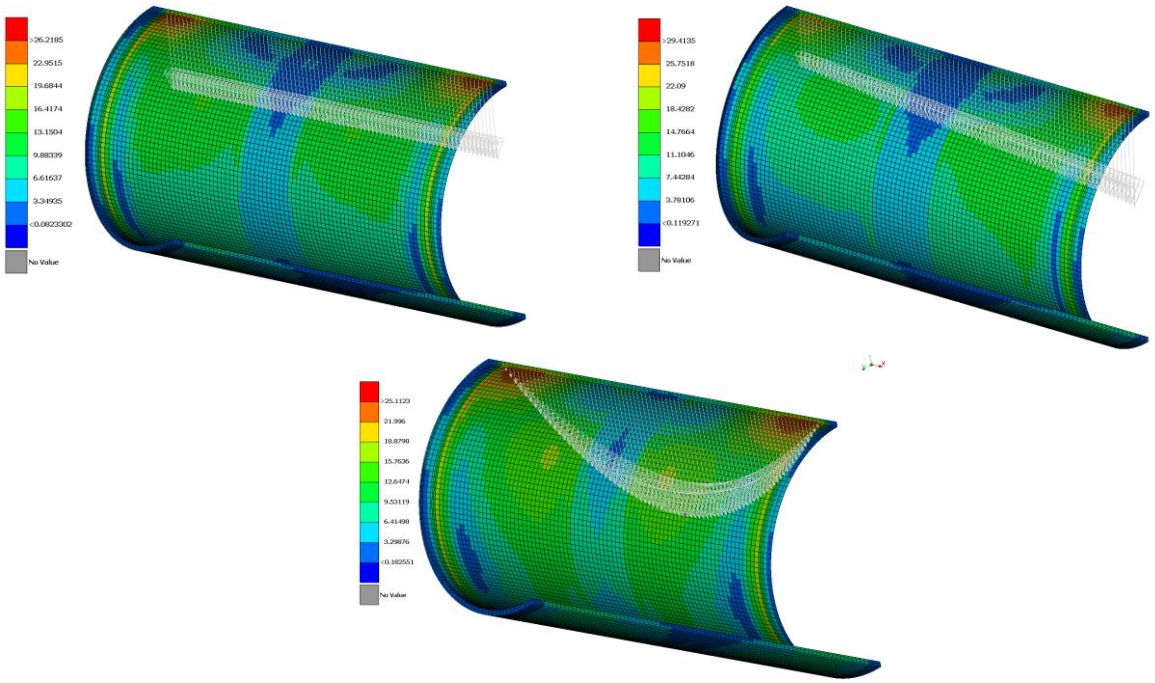

Figure 10 – Stress field dependency along the axis of the drum. The white arrows indicate the loading on a single line, where the maximum loading occurs.

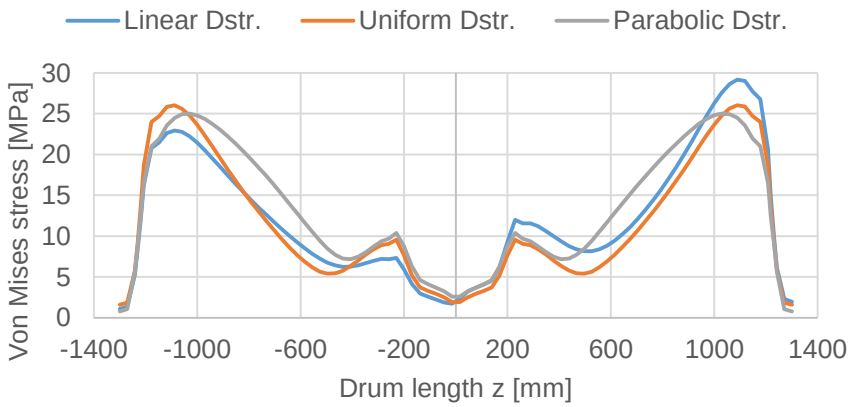

Figure 11 – Stress on the maximum loaded row of elements compared between the three different distribution equations. The parabolic shifts the maximum stressed area towards the centre.

Influence of element type

In Figure 12 the shell of the large model is meshed with two different methods and the same element size. The HEXABLOCK method is more time consuming but provides a much clearer view of the stress, as well as a higher maximum stress for the same element length. In Figure 13, stress on the maximum loaded row of elements is compared between the two types of elements.

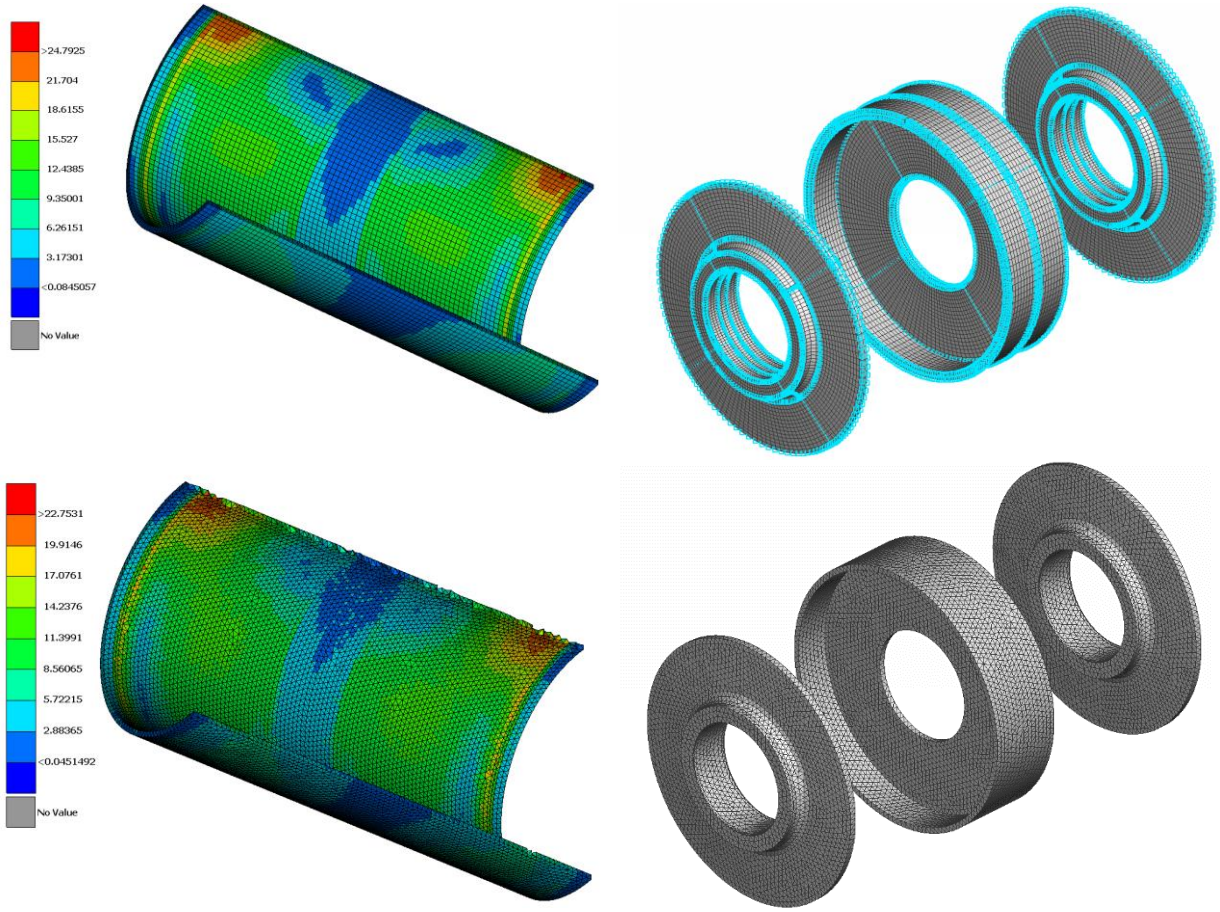

Figure 12 – Stress field comparison between the use of TETRAs and HEXAs. The model is loaded under the same conditions. The HEXAs were created using HEXABLOCK while the shell was meshed with a MAP algorithm.

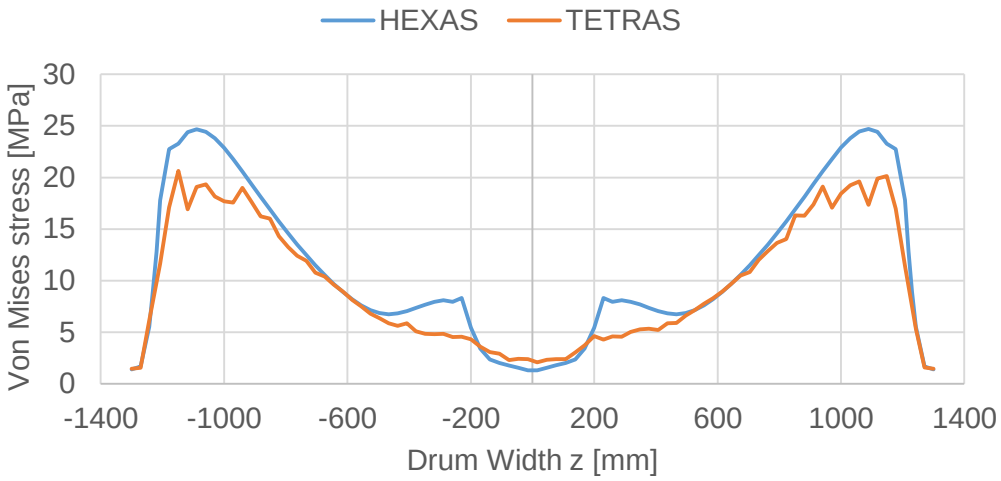

Figure 13 – Stress on the maximum loaded row of elements compared between the two types of elements. The difference in the distribution is pronounced near edges and force path change. The maximum stress is also lower around 20 %.

4. CONCLUSIONS

Usage of 3D elements is the recommended method, as well as modelling of all pulley parts. Compared to the 2D elements the increase in solution time is negligible, while accuracy improves significantly. The preferable 3D element is the HEXA, but at a significant cost

relative to the preparation time. The use of TETRAs is faster but reduces the maximum stress calculated by 20% or higher depending on the position and morphology of the model. Increasing the element density at the areas of interest can result in millions of nodes for a large drum that quickly becomes impractical. Variable density is required to lower the element count and thus the solution time. Selecting the appropriate level of detail at the high stress areas is important for the result reliability. Multiple attempts with different sizes showed that a ratio between radius and element size of about 30-40 has a good convergence.
The load distribution along the axis of drum influences the maximum stress in both size and location. The overall maximum can be up to 15% lower, while for a specific node the decrease can be even higher up to 20%.
The modelling method presented in the current work, provides the basis for a fast tool for calculating the load and the effect of design changes. The incorporation of contact and variable loading coupled with real data covers a broad spectrum of conditions.

ACKNOWLEDGEMENTS

The authors would like to thank BETA CAE Systems, which provides the ANSA and μETA software, and the Public Power Corporation of Greece for their support.

REFERENCES

(1) EURACOAL, Annual Report, 2014.
(2) Lange H., Investigation in Stressing of Conveyor Belt Drums, PhD Thesis, TU Hannover, 1963.
(3) Kalikhman G. L., Umanskii E. S., The influence of a reinforcing ring on the stress distribution in belt conveyor drums, Strength of Materials, 1, 356-363, 1970.
(4) Umanskii E. S., Kalikhman G. L., Experimental investigation of the stress condition in belt conveyor drums, Strength of Materials, 2, 670-673, 1971.
(5) Schmoltzi W., Designing Drums with Transverse Shafts for Belt Conveyors, PhD Thesis, TU Hannover, 1974.
(6) King T. J., The Function and Mechanism of Conveyor Pulley Drums, Paper presented at Beltcon 3 Conference, Johannesburg, 1985.
(7) Sethi V., Nordell L. K., Modern Pulley Design Techniques and Failure Analysis Methods, AIME- SME Annual Convention, Reno, Nevada, 1993.
(8) Qiu X., Sethi V., A New Pulley Stress Analysis Method Based on Modified Transfer Matrix, Bulk Solids Handling, 13(4), 713-724, 1993.
(9) Ravikumar M., Chattopadhyay A. Integral analysis of conveyor pulley using finite element method, Computers & Structures, 71, 303-332, 1999.
(10) Affolter C., Piskoty G., Koller R., Zgraggen M., Rütti T. F. Fatigue in the shell of a conveyor drum, Engineering Failure Analysis, 14, 1038-1052, 2007.
(11) Wegerdt C., Hanel W., Haenel B., Wirthgen G., Zenner H., Seeger T., FKM-guideline, Analytical strength assessment. 5th ed. Frankfurt am Main, VDMA-Verlag GmbH; 2003.
(12) Lill A., Conveyor Pulley Design. Paper presented at Beltcon 14 Conference, Johannesburg, 2007.
(13) BS 7608:1993 Code of practice for Fatigue design and assessment of steel structures
(14) Wang S., Zhang X., Wu K., Sun Y., Finite element analysis for belt conveyor's drum, Advanced Materials Research, 228-229, 764-770, 2011.
(15) Styger G., Laubscher R. F., An investigation into the effect of the manufacturing process on the fatigue performance of conveyor pulleys, Paper presented at Beltcon 16 Conference, Johannesburg, 2011.
(16) Yong-cun G., Zhu-fen W., Kun H., Gang C., Heavy driving drum parametric modelling analysis system development, Applied Mechanics and Materials, 130-134, 641-645, 2012.

(17) Wu Z., Guan W. J., Three-dimensional parametric modelling and finite element analysis of drum on belt conveyer, Applied Mechanics and Materials, 319, 474-476, 2013.
(18) Yuan X., Yang S., Niu Q., Analysis and Design of the Roller for Belt Conveyor Based on ANSYS, Advanced Materials Research, 1027, 315-319, 2014.
(19) ANSA version 12.1.5 User's Guide, BETA CAE Systems S.A., July 2008
(20) μETA PostProcessor version 6.2.0. User's Guide, BETA CAE Systems S.A., June 2008
(21) Kong L, Parker R G (2005). Microslip in flat belt drives. Proc. IMechE, Part C: J. Mech. Eng. Sci., 219, 1097-1106.